FDS simulations and modelling efforts of travelling fires in a large elongated compartment

FDS SIMULATIONS AND MODELLING EFFORTS OF TRAVELLING FIRES IN A LARGE ELONGATED COMPARTMENT

Johan Anderson, Johan Sjöström, Alastair Temple Fire Research, RISE Research Institutes of Sweden, Sweden
Marion Charlier ArcelorMittal Global R&D
Xu Dai, Stephen Welch and David Rush University of Edinburgh, Scotland

ABSTRACT

The present paper investigates a travelling fire scenario in an elongated structure (Length 18 m x width 6 m x height 3 m) with a controlled fire source of six trays filled with diesel (width 4 m x length 0.5 m). The fire spread is controlled manually by initiating fires consecutively in the pools. Fire Dynamics Simulator (FDS) is used to a-priori investigate variations in geometry, material data and fire load whereas simulations using the final design and measured heat release rates (HRR) were performed after the test. The input to the model beside fire source and geometry are thermal material data. The FDS simulations were used to determine the appropriate size of the downstands (2 m from the ceiling in the final design) on the side to create a sufficiently one-dimensional fire spread. The post-test simulations indicate that although there are a lot of variations not included in the model similar results were obtained as in the test.

INTRODUCTION

Structural fire engineering has long been dependent on the assumption of a 'well-mixed reactor' in the fire compartment, meaning that structures are exposed to a fire which is uniform throughout space. The standard fire [1] is a well-known example of this exposure, which is used in fire resistance testing, however other examples do exist and are used for design. Recent work [2-16], promotes travelling fires as a more severe scenario which may occur in large compartments, evidenced by the fires in the World Trade Center towers 1, 2 and 7 (2001); the Windsor tower in Madrid (2006); the Faculty of Architecture building fire at TU Delft (2008); the Interstate bank fire in Los Angeles (1988) and the One Meridian Plaza fire in Philadelphia (1991). The travelling fire methodology divides the fire compartment into two regions, firstly the so-called near field where the fire is burning, and the structure is exposed directly to a moving localized fire. The second region is the so-called far field where the structure is either exposed to preheating because of the developing hot gas layer or is undergoing slow cooling after the fire has passed. Despite these distinct regions, in most examples of analysis done using travelling fires, the convective heat transfer coefficient in the far field is assumed to be constant and at a level equivalent to that used for simulating convective heating under standard fire exposure (a single fire region with a coefficient of ~25 W/(m^2 K)). This contributes to a significant pre-heating of structures prior to exposure to the near field; which may lead to the conclusion that travelling fires can be a more severe design fire for structures. In fact, the convective heat transfer coefficient in the far field is likely to reduce significantly with distance from the near field. This means that the effective preheating will be lower, possibly challenging the assumption of travelling fires as the most severe scenario.

The work presented here is a part of a larger project on travelling fires, the main objectives of the experimental work are to gain information on the behavior of travelling fires in large compartments and the subsequent structural response during fires. More specifically we would like to obtain more information regarding;

1. the optical thickness related to multiple fires travelling along a certain axis, i.e. if the depth of the burning area has an impact on the heat fluxes received by a structural element aligned to the propagation axis.
2. the near field fire exposure to steel structures exposed to travelling fires.
3. the far field fire exposure accounting for radiation from the fire itself and the development of the smoke layer away from the burning area.
4. With the wood crib test additional objectives were added to the task. These were to carry out a test with a natural fire spread in order to:
    a. gain insight on the spread of fire in a compartment.
    b. investigate how changes in local ventilation conditions can change the flame spread rate and fire intensity

In order to achieve these objectives, an experimental campaign with five sets of pool fire tests was conducted in addition to one wood crib test, performed in one elongated compartment. The elongated comparted is chosen to capture an approximately one-dimensional fire. The tests were instrumented such that data is collected regarding, radiation in the far field, gas temperatures throughout the compartment, steel temperatures of the structure, ceiling temperatures, gas velocities, re-radiation to the fuel bed from the smoke layer, flame heights.

A-priori simulations of the outdoor test setup analysing the flows, temperatures under the ceiling as well as the impact on columns exposed to the hot gases were performed. The objective of the model is to identify an empirical relationship between the inputs of ceiling height, distance, heat output, and burning area and the output of convective heat transfer coefficient. In the future, these medium scale tests performed will be used as a validation of this modelling studying the exposure of steel columns to the near field of a travelling fire.

The numerical work was performed using Fire Dynamics Simulation (FDS) version 6.6.0 [17]. The Navier-Stokes equations in the limit of low-speed, thermally-driven flow with an emphasis on smoke and heat transport from fires are solved by the FDS software. The algorithm used is an explicit predictor-corrector scheme that is second order accurate in space and time where turbulence is treated by means of Large Eddy Simulation (LES) of the Deardorff form. This contrasts with other CFD codes for fire safety engineering where Reynolds averaged Navier-Stokes models are used. The heat transfer by radiation is included in the model via the solution of the radiation transport equation for a gray gas. The equation is solved using a finite volume technique for convective transport, thus the name given to it is the Finite Volume Method (FVM). When using 100 discrete angles, the finite volume solver requires about 20 % of the total CPU time of a calculation, a modest cost given the complexity of radiation heat transfer.

This paper presents the results FDS simulations differentiated into two different scenarios, the first is to explore the decrease of the heat transfer coefficient with distance and second, is of travelling fires in a simplified and elongated compartment matching that of the experimental series. The simulations of the second case have been undertaken to support the design of the experimental program and perform simulations matching the experimental conditions after the tests. The a-priori simulations included several variations in the input, such as burner size, heat release rates per unit area, placement of burners, size of downstands and thermal properties of materials. A final design of a steel structure of 18 m length, 6 m wide and 3 m height with a back wall and insulated ceiling was suggested. The degrees of freedom for the two setups are different; the diesel pool fires are controlled by starting the pools fires at certain times (resulting in a prescribed fire spread). There was also a third scenario using wood cribs as fuel. In the wood crib fire test scenario, the wood cribs where ignited at the back wall and allowed to freely develop (resulting in a fire spread influenced by the compartment geometry).

However, the focus of the current work is the modelling of the burner scenario and simulations of the fire spread in the wood cribs will be presented elsewhere. The heat release rates in for the diesel fuel pools are prescribed and the effect of the downstands is studied for different placements of the six pools. In this paper the diesel pool simulations are presented.

CASE 1: A DISCUSSION ON THE HEAT TRANSFER COEFFICIENT

This scenario aims to use computational fluid dynamics, specifically Fire Dynamics Simulator (FDS 6.6) to study the convective heat transfer coefficient directly below a flat surface representing the soffit of a slab in a large compartment. Two models with different heat outputs, 1.2 MW and 6.0 MW, were developed. The model is approximately consisting of floor and ceiling slabs where the ceiling slab with dimensions 8 m × 8 m is located at a height of 3 m, see Figure 1. The model is utilizing a simplified geometry with a square floor area (10m × 10m) and a burner where two different heat release rates are used. The simulation uses a prescribed HRR with an αt^2 growth up to the maximum HRR state after around 400s. The reaction chemistry for the fire is C_2H_3 with soot yield of 0.17g/g. In the model two columns are added to evaluate the heat transfer to obstructions.

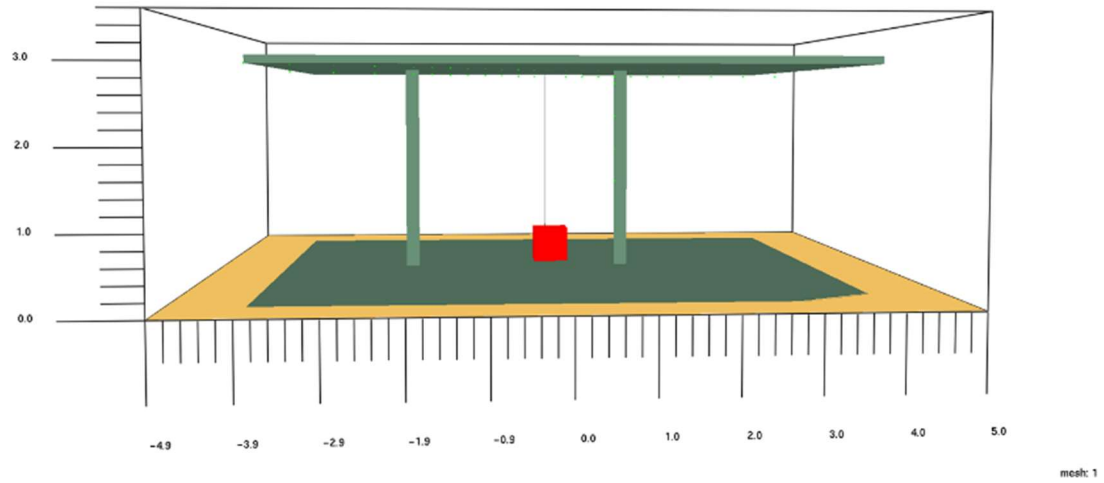

Figure 1. The model as represented in FDS with a cubic fire.

A mesh resolution test with 5cm, 10 cm and 20 cm cells are evaluated and shown in Figure 2 and a significant increase in the temperature is in particular found for the smaller heat release rate with better resolution. For the case with the smaller HRR of 1.2 MW and at distances further out from the centre point of the fire source the difference between the different grids are less pronounced.

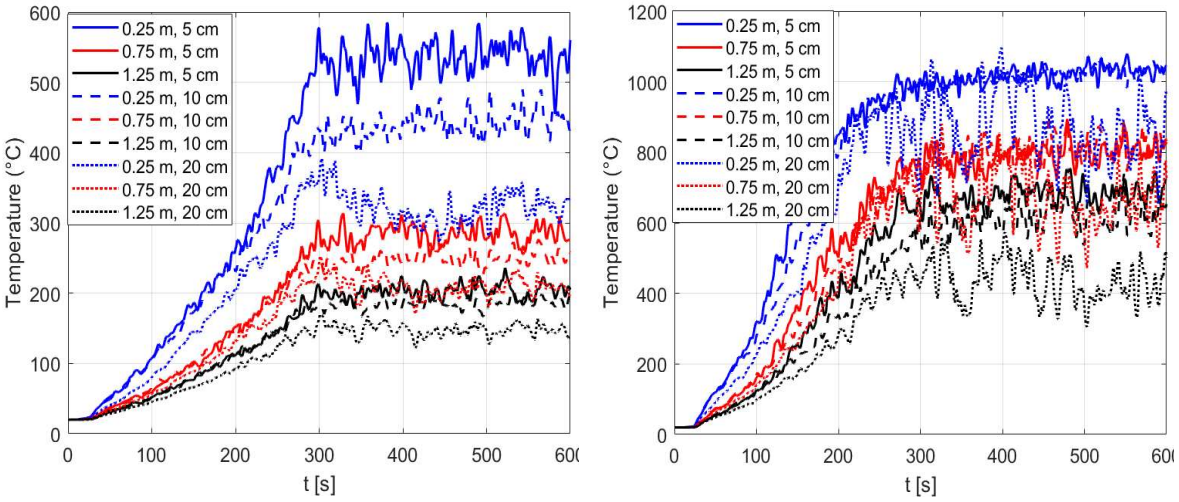

Figure 2. The gas temperature in the cell closest to the ceiling, 1.2 MW (left) and 6 MW (right) averaged over 3s.

However, by increasing the number of cells in the mesh to a resolution of 5 cm only yields small differences from the 10 cm cells in the 6 MW HRR fire case. There are some oscillations found for the 20 cm cells, but the temperatures are quantitatively in the same range at a distance of 0.25 m and 0.75 m of the centre point of the fire source.

It seems likely that the results are well represented by the 5 cm grid at many locations in these two different simulations and in particular for the 6 MW. The heat transfer coefficient will now be evaluated, as it is calculated in FDS.

According the FDS user guide [17] the convective heat transfer coefficient, h, is based on a combination of natural and forced convection correlations:

$$\dot{q}_c'' = h(T_g - T_w) \text{ W/m}^2; \qquad h = max\left(C|T_g - T_w|^{1/3}\left|\frac{k}{L}Nu\right.\right) \text{ W/(m}^2\text{ K)}$$

where C is an empirical coefficient for natural convection (1.52 for a horizontal plate and 1.31 for a vertical plane or cylinder), L is a characteristic length related to the size of the physical obstruction, and k is the thermal conductivity of the gas. The Nusselt number (Nu) depends on the geometric and flow characteristics. For many flow regimes, it has the form:

$$Nu = C_1 + C_2 Re^n Pr^m ; \qquad Re = \rho|u|L/\mu ; \qquad Pr \approx 0.7$$

For planar and cylindrical surfaces, the default values are $C_1 = 0$, $C_2 = 0.037$, $n = 0.8$, $m = 0.33$, and $L = 1$ m. For spherical surfaces, the default values are $C_1 = 2$, $C_2 = 0.6$, $n = 0.5$, $m = 0.33$, and $L = D$, the diameter of the sphere.

The numerically computed heat transfer coefficients are shown in Figure 3.

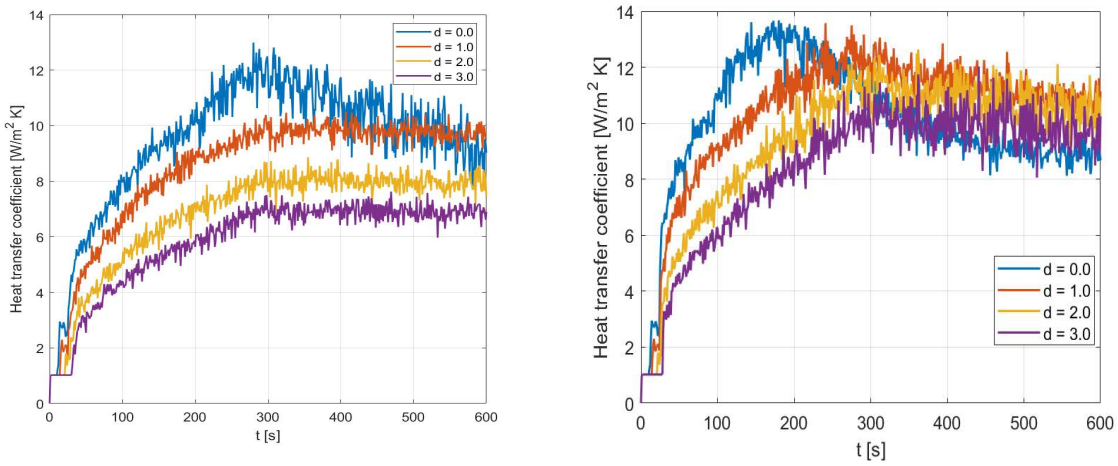

Figure 3. The heat transfer coefficient (h) to the ceiling as a function of the distance (d) for 1.2 MW (left) and 6 MW (right) for the 5 cm grid.

We first note that in general the computed heat transfer coefficient to the ceiling in FDS are much lower than the often-used value of 25 W/(m^2 K), even very close to the fire source. In addition, it is found that the heat transfer coefficient decreases quite rapidly with distance from the centre point of the fire source, as is seen for the 1.2 MW case whereas this effect seems not to be present for the 6 MW fire. Furthermore, directly above the fire source in both simulations the heat transfer coefficient first rapidly increases with the increasing HRR in the simulation whereas later in the simulation where the HRR saturates the heat transfer coefficient decreases. The heat transfer models included in FDS have been studied in Ref. 18, in wide range of different cases. Validation results regarding the convective heat flux was presented in Section 12.4 of Ref. [18].

CASE 2: MODELLING AND MESH RESOLUTION

In the Case 2 test set-up simulation, a model spanning width 6m × length 18m × height 3m as shown in Figure 4 is used. The travelling fire scenario is modelled with six trays filled with diesel where each of them burns with a pre-determined Heat Release Rate (HRR), see Figure 5, the prescribed Heat Release Rate per Unit Area (HRRPUA) is 873 kW/m^2 for each tray. The HRRPUA is estimated from mass loss rates of approximately 0.05 kg/m^{2}s with 0.8 combustion efficiency and using reduction factor due to the thinness of the burners of 0.5. The reaction N-decane model preprogrammed into FDS is used as reaction chemistry with a soot yield of 0.05 g/g [17]. Each fire increases from 0 to 1746 kW in 120 s and is then kept at 1746 kW for 520 s whereafters the HRR is decreased to 0 in 120 s, creating a slowly oscillating total HRR with a mean of approximately 1600 kW for a duration of 30 minutes. The trays are 4.0 m wide and 0.5 m in the direction along the structure, see Figure 4. The trays are placed 1.0 m from each of the sides and the first tray is placed 0.5 m from the back wall with a spacing of 1.5 m between trays. Note that the tray closest to the back wall is not used in these simulations.

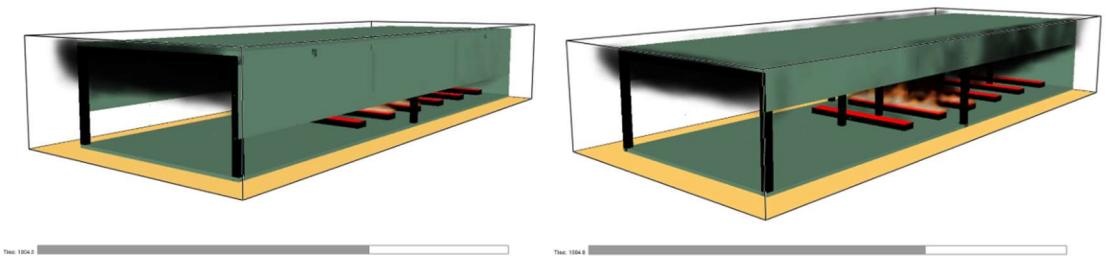

Figure 4. FDS domain as shown during a diesel fuel simulation with two different downstands.

The main structure consists of steel downstands, sandwich panels with steel sheet and mineral wool insulation in the ceiling, steel columns and a concrete floor as shown in Figure 4. The thermal properties of the materials used in the simulations are presented in Table 1.

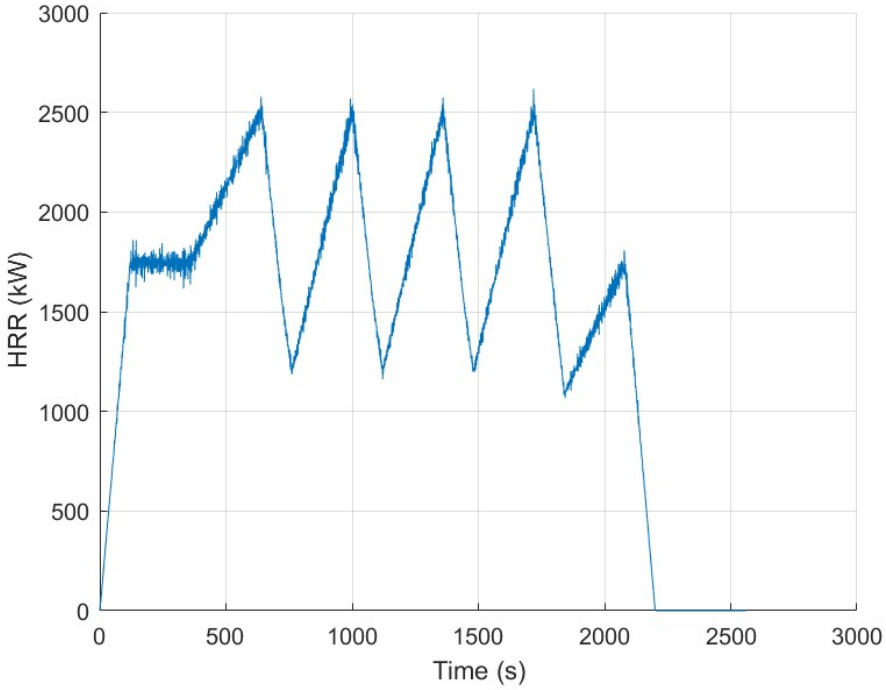

Figure 5. The HRR as specified in the a-priori simulations.

Material\Properties	Conductivity [W/mK]	Density [kg/m^3]	Specific heat [J/gK]	Emissivity [-]
Steel	45.8	7850	0.46	0.95
Concrete	0.4	2400	0.96	0.85
Mineral Wool	0.04	75	0.84	0.9

Table 1. Material properties used in the simulations.

To assess the different cases a few measurement devices, namely thermocouples (TCs), bi-directional probes (BD-probes) for measuring the velocities and plate thermometers (PTs), were included in the model in the same places as in the real tests. When including plate thermometers in an FDS model describing a transient scenario the response time of the measurement device must be considered, i.e. a

thermal model for plate thermometers is needed [19-20]. In the model used in the present study, temperature dependent thermal properties of the components in the plate thermometer were used. The plate thermometer included a metal sheet of Inconel 600 and insulation material in the same manner as in Ref. [19].

One important aspect in defining simulations is resolving the conflict between their overall accuracy and the computational time required for them to run. The simulation must have a sufficiently resolved mesh to provide accuracy while the finer the mesh size the more processing time required to run. To help resolve this a mesh resolution study was performed using 20 cm, 10 cm and 5 cm cubic grids. A general recommendation for the mesh size relevant for buoyant plumes is to compute the ratio characteristic fire diameter (D*) and the nominal grid size (dx), where the recommended range is $10 < D^*/dx < 20$. The ratio is found to be 5.78, 11.56 and 23.11 for 20 cm, 10 cm and 5 cm grid, respectively. Other indicators of flow resolution are to monitor the measurement of turbulence resolution and the wavelet error. It is concluded that the 10 cm grid gives sufficiently good resolution where the measurement of turbulence resolution is below 0.2 at most points in time and space except for some spikes well localized in time, a similar result if found in the case of the wavelet error whereas the 20 cm grid is deemed to be to coarse to yield accurate results. The time to perform the simulations are roughly 10 h, 4 days, 3 weeks on a Linux cluster dividing the volume into 3 meshes, respectively for the three mesh sizes. Thus, in the remainder of the paper only results computed using a mesh resolution of 10 cm is presented.

A-PRIORI SIMULATIONS OF TEST SETUP

The purpose of the a-priori simulations was to investigate the influence on the results of certain parameters such as tray size and downstand. In this paper we present only those simulations that are close to the final experimental set-up, see Table 2 where a summary of the simulations is presented.

Simulation	Tray length, area, $P_{max,\,burner}$	Downstand
1	4 m, 2 m^2, 1746 kW	2 m
2	4 m, 2 m^2, 1746 kW	1 m

Table 2. The a-priori simulation set-up variations.

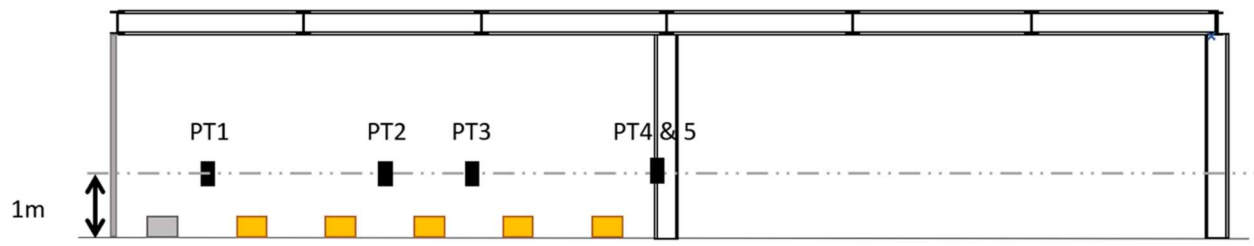

Figure 6a. The placement of thermocouples (TCs) , plate thermometers (PTs) and bi-directional (BD)-probes along the structure with the back wall to the left and the fire trays indicated in orange.

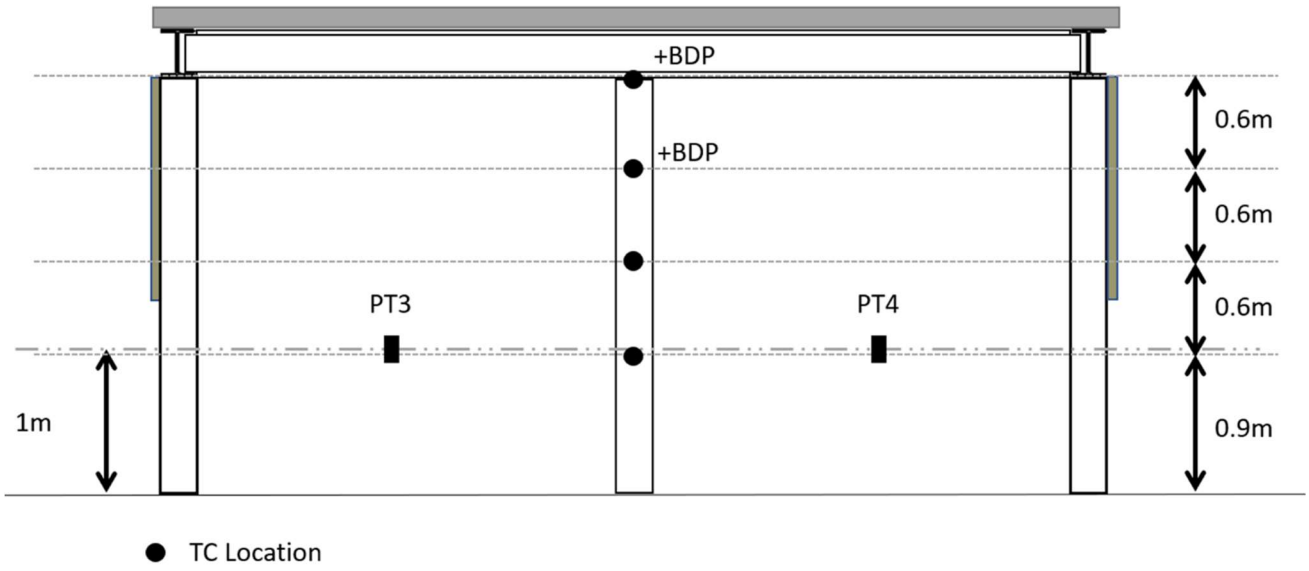

Figure 6b. The placement of thermocouples (TCs), plate thermometers (PTs) and bi-directional (BD)-probes across the structure 9 m from the back wall.

Figure 6c. A figure of test setup and live test.

The large-scale test built according to Figure 6a and 6b indicating the size is shown in a picture taken during the test as shown in Figure 6c. The placement of measuring points are found in Figures 6a and b and the main results of the a-priori investigation are shown in Figure 7, 8 and 9. In Figure 7, the gas temperatures (moving averages of 10 s) computed by the thermocouple function in FDS for a 0.5 mm device. The thermocouples (TCs) are positioned beside the middle column halfway along (9.0 m from the back wall) the structure as seen on Figure 6b at heights 2.4 m (TC 1), 2.1 m (TC 2), 1.5 m (TC 3) and 0.9 m (TC 4) above ground. The effect of the downstands a clearly visible where significantly lower temperatures for TC 1 and TC 2 are found in the case with shorter downstands, 1.0 m instead of 2.0 m, whereas much more similar temperatures are found closer to the ground where the air entrainment is similar.

The flow velocities (moving average of 60 s) at two heights (2.4 m and 2.1 m) by the middle column, see Figure 6b are shown in Figure 8. A positive flow is moving away from the back wall. The rather different flow dynamics is clearly visible in the two cases where higher flow rates are found for the shorter downstands due to more entrainment of air from the sides and not only flow along the structure. Note the time variation in the velocity where in particular in Sim 2 an almost constant flow moving the combustion gases along the structure and then suddenly decreasing due to the impact of the closest pool fire.

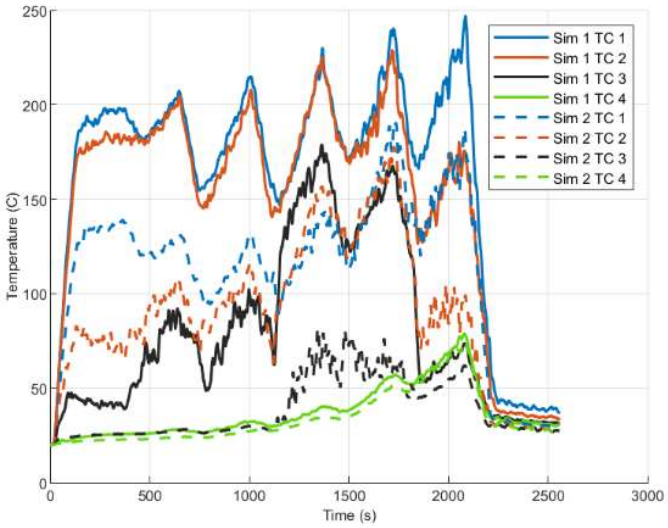

Figure 7. The thermocouple temperatures for simulations 1 and 2 at four positions.

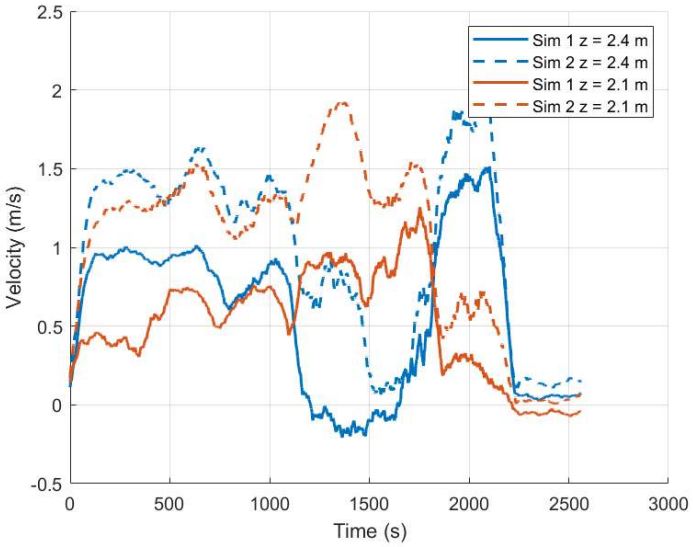

Figure 8. The velocity along the structure at two positions for simulations 1 and 2.

In Figure 9, the temperatures (moving averages of 10 s) computed by the plate thermometer (PT) model are shown at five locations. The plate thermometers are placed at 1.0 m from the floor at the centre line along the structure and 1.5 m (PT 1), 4.5 m (PT 2), 6.0 m (PT 3) from the back wall. PT 4 and PT 5 are placed 9.0 m from the back wall and symmetrically 1.5 m from the centre line, see Figure 6b. Note that since the tray closest to the back wall is not used the temperature of PT 1 is much lower compared to PT 2 and PT 3 which shows a clear peak for maximum intensity of the closest pool fire. Note, that the plate temperatures are much less influenced by the changing the downstands.

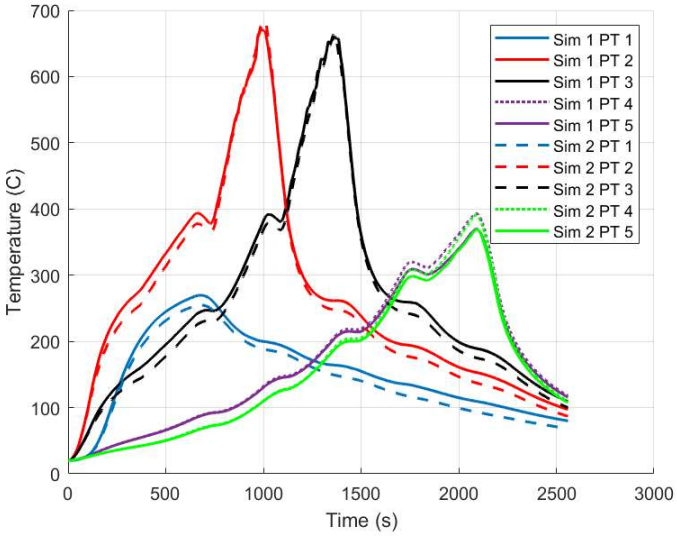

Figure 9. The temperatures measured by the modelled PTs at five positions.

A-POSTERIORI SIMULATIONS OF TEST SETUP

After the tests were performed the HRR, presented in Figure 7, of the trays in the test were estimated by flame height observations and then scaled to match the total energy from the fuel burnt (assuming a combustion coefficient of 0.8) with the same reaction chemistry as in the a-priori

simulations. The Heskestad's relationship of pool fire flame heights to HRR was used, however the test scenario is outside the validity limits of the Heskestad's correlation due to the specific geometry of the pools. (the pools are too elongated, and the relative proximity of the ceiling may also impact the experimental correlation used). We conclude that this estimate can only provide a relative intensity of the fire with time. Furthermore, note that only five of the six burners were used in the actual test series, where the tray closest to the backwall was not used. It is interesting to investigate similarities and differences in the dynamics between the model and the test, thus in the rest of this paragraph comparisons between test results of test 4 and the analogous simulation is presented. In Figure 7, the estimated HRR is shown for simulation of test 2 (blue solid line), simulation of test 4 (red solid line) and test 4 (black dashed line). The HRR is estimated for each burner individually however in the simulation at certain points in time there are several burners active and thus the HRR in the test and simulation does not exactly match at those locations.

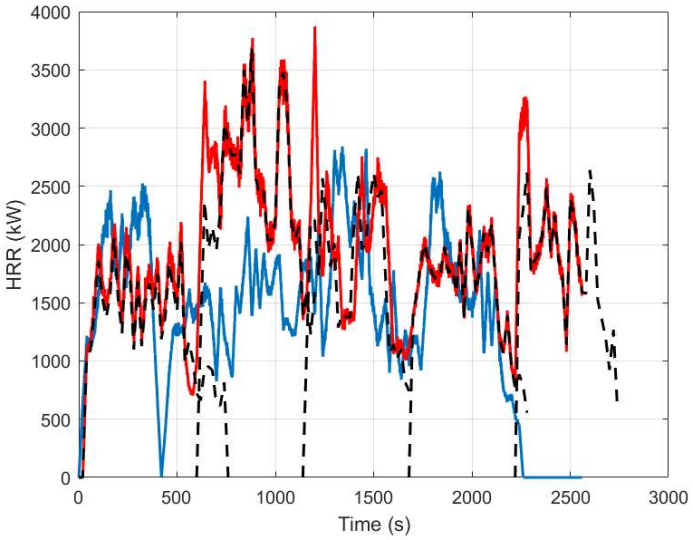

Figure 10. The HRRs of simulation 3 (blue line) and 4 (red line) representing the test 2 and 4 (black line) in the experimental series.

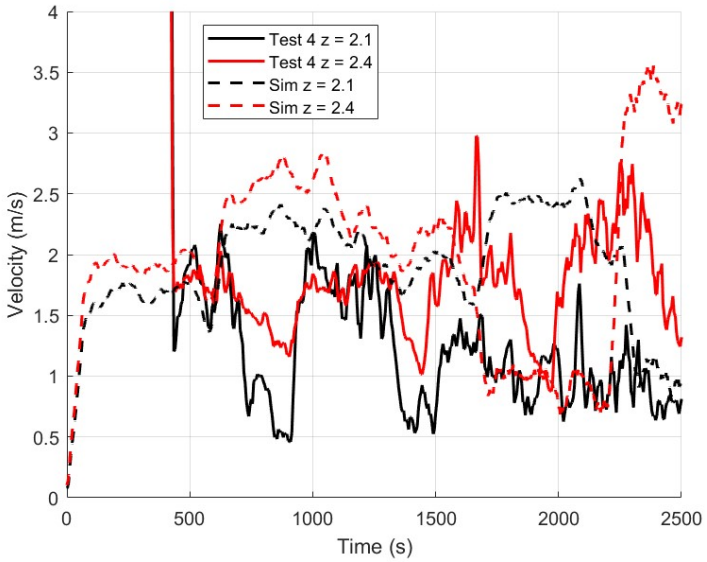

Figure 11. The velocity along the structure at two positions for test 4 and simulation of test 4.

In Figure 11, the flows along the structure are displayed by the centre column, i.e. 9 m from the back wall. Although, there are differences in the precise values of the flows they are often of the same order however there are significantly larger fluctuations in the measured velocity which may come from wind, uncertainties in the temperature measurements or estimation of the Reynolds number.

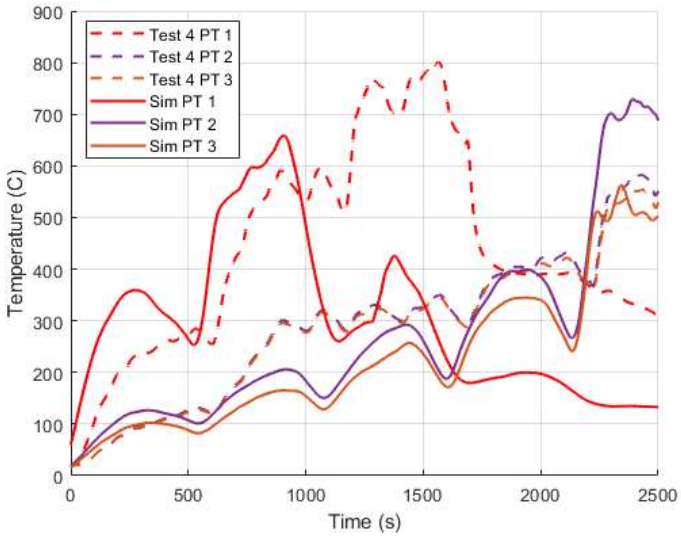

Figure 12. A comparison of the temperatures measured by the plate thermometers (PTs) between test 4 and the simulation of test 4.

The response of the plate thermometers can be seen in Figure 12. They were placed at 1.2 m from the floor along the centre line of the structure and at distances of 4.5 m and 6.0 m from the back wall for PT 1 and 2 respectively. PT 3 and PT 4 were both placed 9.0 m from the back wall and symmetrically 1.5 m from the centre line, see Figure 6b. Quantitatively similar temperatures are found for the PT 1 and PT 2 whereas lower temperatures are found for the plate thermometers placed symmetrically 1.5 m from the sides. It is observed that the measured temperature can be significantly higher than the computed temperature in the simulation, after approximately 1000 s into the test where the measured temperature is almost 400 °C higher. There are several possible reasons for this discrepancy, it should be noted that the HRR is estimated indirectly by visual means and thus there is some uncertainty in the precise time development of the fire as well as the climate conditions with effect of wind could play a role. It is most likely that these are influenced by the cold air coming in from the sides.

DISCUSSIONS

It has been recognized in structural fire engineering that travelling fires may have a significantly different impact on structures affected by fires compared to the older room fire models and the scenarios covered by standardized testing. Thus, it is of interest to investigate this challenge, both experimentally and by numerical work to be able to elucidate on the physics involved in the process. In the present work Computational Fluid Dynamics (CFD) simulations are used to suggest a test setup for travelling fires and in a later stage used for evaluation of the performed tests. The modelling work utilized CFD software FDS 6.6.0. As a background for the travelling fire model assumption of a rather large heat transfer coefficient a series of simulations of decrease of the heat transfer coefficient with distance was performed. It was evident that from these simulations, the heat transfer coefficient decreases rapidly with distance as available heat and flows diminished, in all cases far below the recommended 25 W/(m^2 K). The suggested test setup is an elongated structure, 18 m

long, 6 m wide and 3 m high with a back wall, where the fire source is diesel distributed in six pans that can spread at different rates as controlled by the ventilation on the sides and size. A mesh resolution test suggested that to have good enough accuracy a 10 cm x 10 cm x 10 cm grid is sufficient, although a 5 cm x 5 cm x 5 cm grid would give slightly more reliable results the number of simulations would be impeded since these simulations would take more three weeks each. In the simulations several different options were considered such as varying maximum HRRPUA, investigating different sizes and placement of diesel pans, varying downstands on the sides controlling the air entrainment and thermal properties of the materials. It can be concluded that the main variations that influence the dynamics are the placement of pans and the downstands. It is shown that significantly lower gas temperatures can be found for the shorter downstands (1.0 m instead of 2.0 m). The final design includes the longer downstands to enhance the one-dimensional structure of the fire. The tests performed in the final design are then evaluated by post-test simulations using the measured HRR from the tests. The comparisons are focused on Test 4 where velocities measured by BD-probes and temperatures measured by thermocouples and plate thermometers can be compared. It is found that, although there are differences, there are quite a few similarities in the maximum temperatures obtained and the quantitative flow speeds found. Simulations can therefore be further utilized to understand the dynamics in travelling fire situations. In this work, there are two main objectives with the simulations in the current work. Firstly, the simulations were used to design the test set-up, dimensions, size, number and placements of the burners, the size of the downstands. Secondly, the post-test simulations were used to further investigate the dynamics of fire and verify the almost one-dimensional character of the test setup. In the future, simulations of the wood crib tests will be performed and the results in addition to the experimental results may be used to evaluate the temperatures on the structural components.

ACKNOWLEDGEMENT

This work was carried out in the frame of the TRAFIR project with funding from the Research Fund for Coal and Steel (grant N°754198). Partners are ArcelorMittal Belval & Differdange, Liège University, the University of Edinburgh, RISE Research Institutes of Sweden and the University of Ulster.

REFERENCES

[1] ISO 834-1:1999. Fire-resistance tests - Elements of building construction - Part 1: General requirements.

[2] Abecassis, C., Abecassis-Empis, C., Reszka, P., Steinhaus, T., Cowlard, A., Biteau, H., Welch, S., Rein, G. & Torero, J.L. (2007). Characterisation of Dalmarnock fire Test One. Experimental Thermal and Fluid Science, 1334-1343.

[3] Harmathy, T.Z. (1972). A new look at compartment fires. Fire Technology, 8(3), 196-217.

[4] Dai, X. Welch, S. & Usmani, A. (2017) A critical review of 'travelling fire' scenarios for performance-based structural engineering, Fire Safety Journal, vol. 91, pp. 568–578.

[5] Welch, S., Jowsey, A., Deeny, S., Morgan, R. & Torero, J.L. (2007). BRE large compartment fire tests—Characterising post-flashover fires for model validation. Fire Safety Journal, 548-567.

[6] Zhen, H. (2014) Computational modelling of fire spread in a full-scale compartment fire test, IMFSE thesis, School of Engineering, University of Edinburgh

[7] B.R. Kirby, D. W. (1999). NATURAL FIRE IN LARGE SCALE COMPARTMENTS, International Journal on Engineering Performance- Based Fire Codes, 1(2), 43-58.

[8] Rush, D, Lange, D, Maclean, J & Rackauskaite, E (2015). Effects of a travelling fire on a concrete columns - Tisova Fire Test, Paper presented at Applications of Structural Fire Engineering, Dubrovnik, Croatia, 15/10/15 - 16/10/15.

[9] Rackauskaite, E., et. al. (2015). Improved formulation of travelling fires and application to concrete and steel structures. Structures, 3, 250-260.

[10] Rackauskaite, E., et al, (2017). Structural analysis of multi-storey steel frames exposed to travelling fires and traditional design fires. Engineering Structures, 271-288.

[11] Horová, T., (2013). Temperature heterogeneity during travelling fire on experimental building. Advances in Engineering Software, 119-130.

[12] Stern-Gottfried, J., Rein, G., (2012). Travelling fires for structural design–Part I: Literature review; Fire Safety Journal 54, 74-85.

[13] Stern-Gottfried, J., Rein, G., (2012) Travelling fires for structural design–Part II: Design methodology; Fire Safety Journal 54, 96-112.

[14] Gann, R. G., (2005). Hamins, A., McGrattan, K.B., Mulholland, G.W., Nelson, H.E., Ohlemiller, T.J., Pitts, W.M., Prasad, K.R. (2005). Reconstruction of fires in the World Trade Centre Towers. NIST NCSTAR, 1-5.

[15] Degler, J., Eliasson, A., Anderson, J., Lange, D. and Rush, D., A-priori modelling of the Tisova fire test as input to the experimental work, The First International Conference on Structural Safety and Blast (CONFAB), Glasgow, Scotland, UK (2015), pp. 429–438

[16] Charlier, M., Gamba, A., Dai, X., Welch, S., Vassart, O., Franssen, J.-M., CFD analyses used to evaluate the influence of compartment geometry on the possibility of development of a travelling fire, Proceedings of the 10th International Conference on Structures in Fire, Belfast, UK (2018), pp. 341-348

[17] McGrattan, K., Hostikka, S., Floyd, J., McDermott, R., Vanella, M. Fire Dynamics Simulator (Version 6) – user's guide. NIST Special Publication 2019.

[18] McGrattan, K., McDermott, R. Hostikka, S. Floyd, J., Fire Dynamics Simulator Technical Reference Guide Volume 3: Validation, NIST Special Publication 2019.

[19] Anderson, J., Jansson, R., Boström, L., Milovanović, B., (2018). Modeling of fire exposure in facade fire testing, Fire and Materials 42 (5), 475-483.

[20] Anderson, J., Jansson, R., Boström, L., Milovanović, B., (2018). Experimental comparisons in façade fire testing considering SP Fire 105 and the BS 8414-1, Fire and Materials 42 (5), 484-492.